Bioorganic & Medicinal Chemistry Letters 23 (2013) 2787–2792

Contents lists available at SciVerse ScienceDirect

Bioorganic & Medicinal Chemistry Letters

journal homepage: www.elsevier.com/locate/bmcl

Structure-based design, SAR analysis and antitumor activity of PI3K/mTOR dual inhibitors from 4-methylpyridopyrimidinone series

Hengmiao Cheng [a,*], Jacqui E. Hoffman [a], Phuong T. Le [a], Mason Pairish [a], Robert Kania [a], William Farrell [a], Shubha Bagrodia [b], Jing Yuan [b], Shaoxian Sun [b], Eric Zhang [c], Cathy Xiang [c], Deepak Dalvie [c], Sadayappan V. Rahavendran [c]

[a] Cancer Chemistry, Pfizer Worldwide Research and Development, La Jolla Laboratories, 10770 Science Center Drive, San Diego, CA, 92121, USA
[b] Oncology Research Unit, Pfizer Worldwide Research and Development, La Jolla Laboratories, 10770 Science Center Drive, San Diego, CA, 92121, USA
[c] PDM, Pfizer Worldwide Research and Development, La Jolla Laboratories, 10770 Science Center Drive, San Diego, CA 92121, USA

ARTICLE INFO

Article history:
Received 15 December 2012
Revised 23 January 2013
Accepted 1 February 2013
Available online 13 February 2013

Keywords:
SBDD
Kinase inhibitor
PI3K/mTOR dual inhibitor
Cancer
Antitumor
Effective polar surface area
ePSA
Metabolite

ABSTRACT

PI3K, AKT and mTOR, key kinases from a frequently dysregulated PI3K signaling pathway, have been extensively pursued to treat a variety of cancers in oncology. Clinical trials of PF-04691502, a highly potent and selective ATP competitive kinase inhibitor of class 1 PI3Ks and mTOR, from 4-methylpyridopyrimidinone series, led to the discovery of a metabolite with a terminal carboxylic acid, PF-06465603. This paper discusses structure-based drug design, SAR and antitumor activity of the MPP derivatives with a terminal alcohol, a carboxylic acid or a carboxyl amide.

© 2013 Elsevier Ltd. All rights reserved.

The phosphatidylinositol 3-kinase (PI3K) signaling pathway plays crucial roles in cell growth, proliferation and survival, and is a frequently dysregulated pathway in human cancers.[1,2] Inhibitors of key kinases in the pathway, including PI3K, AKT and mTOR, have been extensively pursued in oncology in recent years.[3] In order to effectively block the PI3K pathway, overcome feedback loops,[4] and block PI3K independent mTOR activation, our strategy to target PI3K signaling pathway is focused on pursuing PI3K/mTOR dual inhibitors. PF-04691502 is a highly potent and selective ATP competitive kinase inhibitor of class 1 PI3Ks and mTOR, and has progressed to phase I/II clinical trials for the treatment of solid tumors (see Fig. 1).[5,6]

PF-04691502, derived from 4-methylpyridopyrimidinone (MPP) series, exhibited potent in vitro activity against class I PI3K isoforms and mTOR, with mPI3Kα K_i of 0.57 nM (mouse PI3Kα was used as a surrogate of human PI3Kα in the primary screening), and mTOR K_i of 16 nM. In a BT20 cell assay, measuring inhibition of AKT phosphorylation at S473, PF-04691502 exhibited excellent cellular potency with an IC_{50} of 13 nM. Co crystal structure of PF-04691502 bound in PI3Kγ was determined (Fig. 2).[5] The aminopyrimidine formed key hydrogen bonds with the hinge residue, Val 882. The methyl at the 4 position on the MPP core fit tightly in a small hydrophobic pocket unique to PI3K and mTOR, conferring excellent kinase selectivity for the MPP derivatives. The ring nitrogen on the methoxypyridine formed a key hydrogen bond with a conserved water molecule in the selectivity pocket. The terminal alcohol of the hydroxyethyl formed an intramolecular H bond with the ether oxygen atom off the cyclohexyl ring, reducing the effective number of hydrogen bond donors, and helping the compound to achieve excellent permeability and cellular potency.

Structural analysis also revealed that the terminal alcohol was located in a solvent exposed region surrounded by polar residues, and there was space between the terminal alcohol and the polar residues. Modeling studies, exemplified by docking **29** in PI3Kγ as illustrated in Figure 3, indicated a primary carboxyl amide would fit in the space, with the amide carbonyl pointing towards the solvent, and an intramolecular H bond between the amide N–H and the ether oxygen could be formed. In PF-04691502 co crystal structure with PI3Kγ, the Lys 833 side chain was pointing down as shown in Figure 2, and there was no H bond interaction between MeO-pyridine and Lys 833. However, the F atom on the 4-MeO-5-F-3-pyridine in **29** pushed Lys 833 up and inward as illustrated in Figure 3, the terminal amino group from Lys 833 side

* Corresponding author.
E-mail address: henry.cheng@pfizer.com (H. Cheng).

0960-894X/$ - see front matter © 2013 Elsevier Ltd. All rights reserved.
http://dx.doi.org/10.1016/j.bmcl.2013.02.020

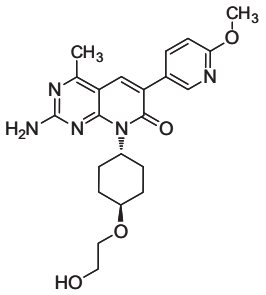

PF-04691502

Figure 1. Chemical structure of PF-04691502.

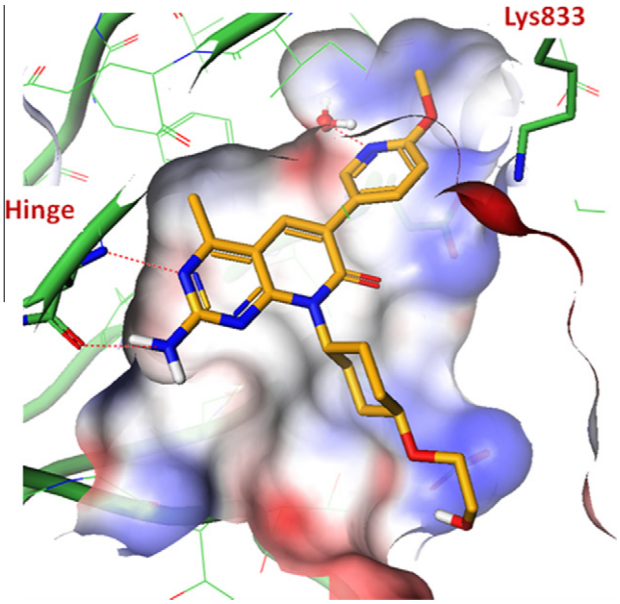

Figure 2. Co crystal structure of PF-04691502 bound in PI3Kγ.

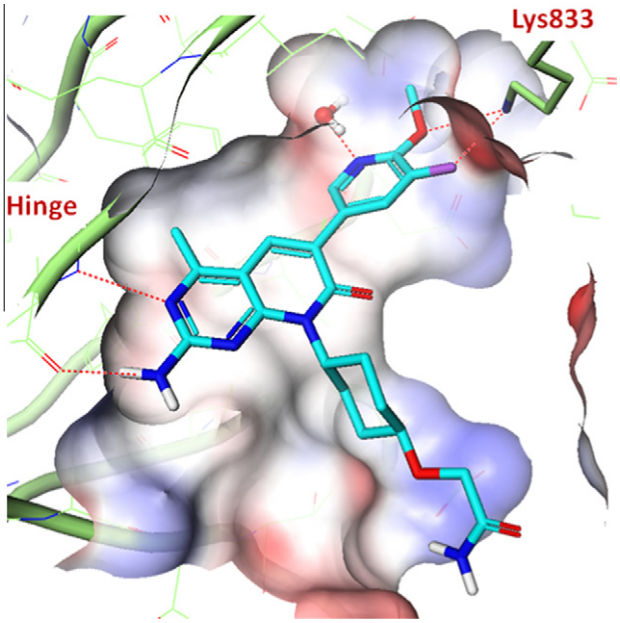

Figure 3. Amide derivative **29** modeled in PI3Kγ.

chain was in close distance to form H bonds with both the oxygen atom and the F atom. The H bond interaction between the conserved water molecule and the pyridine ring N was retained. The interaction between 4-MeO-5-F-3-pyridine and Lys 833 and the conserved water molecule was recently reported both for a modified MPP derivative[7] and for AMG 511, in which 4-MeO-5-F-3-pyridine was attached to a different scaffold.[8] Based on the modeling studies, we decided to investigate the SAR by replacing 4-MeO-3-pyridine in PF-04691502 with different heteroaryl groups including 4-MeO-5-F-3-pyridine. In addition, the terminal amide derivatives had much higher Topological Polar Surface Area (PSA) than the terminal alcohol derivatives such as PF-04691502, so we were interested in comparing the SAR between the amides and the alcohols, for example, binding affinities with mPI3Kα and mTOR, correlation between PSA, LogD, permeability and cellular potency.

Illustrated in Scheme 1 is the synthetic route for preparing MPP derivatives with cis-cyclohexyl moiety substituted at the 8 position; the *trans*-cyclohexyl derivatives were prepared by using the corresponding *trans*-4-aminocyclohexanol at step 1.[9] Compound **1** was reacted with *cis*-4-aminocyclohexanol to produce compound **2**, which was reacted with *tert*-butyl bromoacetate, followed by quenching with MeOH to give the isolated methyl ester **3**. The ester in **3** was reacted with ammonia to yield compound **4**, which was reacted with hydroxylamine in ethanol to generate compound **5**. Palladium-catalyzed coupling of **5** with ethyl acrylate yielded compound **6**, which was subjected to intramolecular cyclization to generate compound **7**. Bromination of **7** with NBS, followed by Suzuki coupling reactions with an appropriate bronic acid or bronic ester gave the desired product **9**.

To assess the metabolic profile of PF-04691502 in humans in vivo, the plasma obtained from patients dosed with PF-04691502 at 8 mg QD in a clinical pharmacology dose escalation study was analyzed.[10] The high dose was selected for metabolite profiling to ensure that all metabolites were detected in the human plasma. The total ion chromatogram of plasma showed 4 peaks. The retention times and the molecular ions of the peaks at 24.81 and 26.80 min were identical to the PF-04447949[11] and unchanged PF-04691502, respectively (Fig. 4). The additional peaks at 25.24 min (M2) and 29.07 (M6) showed molecular ions at *m*/*z* 602.2 and 440.19. The fragmentation pattern of the two molecular ions suggested the M2 and M6 were the glucuronide conjugate of PF-04691502 and the carboxylic acid metabolite, respectively (Fig. 5). Although the site of conjugation was unknown, the formation of M2 involved catalysis by uridine glucuronyl transferase (UGT). On the other hand, the formation of M6 was mediated by oxidation of the alcohol either by CYP450 or via alcohol dehydrogenase to the aldehyde that was oxidized to the corresponding acid, ({*trans*-4-[2-amino-6-(6-methoxypyridin-3-yl)-4-methyl-7-oxopyrido[2,3-*d*]pyrimidin-8(7*H*)-yl]cyclohexyl}oxy)acetic acid (M6, PF-06465603) (Scheme 2). The identity of M6 was further confirmed by comparison of its mass spectrum and retention time with an authentic standard, which was prepared from PF-04691502 by oxidizing the primary alcohol to the acid (Scheme 3)

MPP derivatives with different heteroaryl groups off the 6 position, with *cis* or *trans*-cyclohexyl off the 8 position, and with terminal alcohol or terminal amide were prepared following the synthetic route described in Scheme 1. The in vitro potency, calculated SFLogD, HLM in vitro clearance, permeability (RRCK), and PSA for the alcohol and amide derivatives, and the metabolite **10** are summarized in Table 1.

In the mPI3Kα assay, compounds with six-membered heterocycle are in general more potent than those with 5 or 10-membered heterocycles as shown in Figure 6, suggesting six-membered heterocycle fits the best in PI3Kα binding site. Modeling studies with **29** indicated that the F atom could help position Lys 833 side chain to form H bonds with both the oxygen atom and the F atom of the

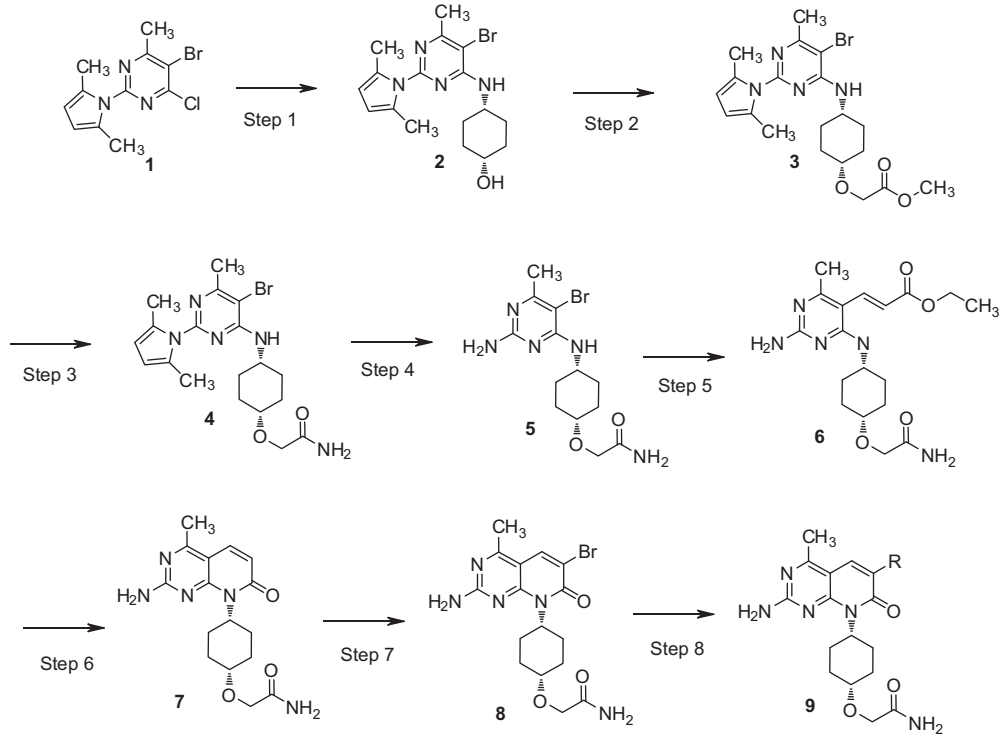

Scheme 1. Synthesis of amide derivatives. Reagents and conditions: (1) *cis*-4-aminocyclohexanol, diisopropylethylamine, DMF, yield: 82%; (2) (a) *tert*-butyl bromoacetate, NaH, THF, (b) MeOH, yield: 37%; (3) ammonia in methanol; (4) NH_2OH hydrochloride, EtOH/water, reflux, yield: 50% over two steps; (5) ethyl acrylate, $Pd(PPh_3)_4$, triethylamine, yield: 69%; (6) PhSH, NsAPh, DBU, DIEA, yield: 89%; (7) NBS, DMF, yield: 97%; (8) boronic acid, K_2CO_3, $Pd(PPh_3)_2Cl_2$, DMF–water.

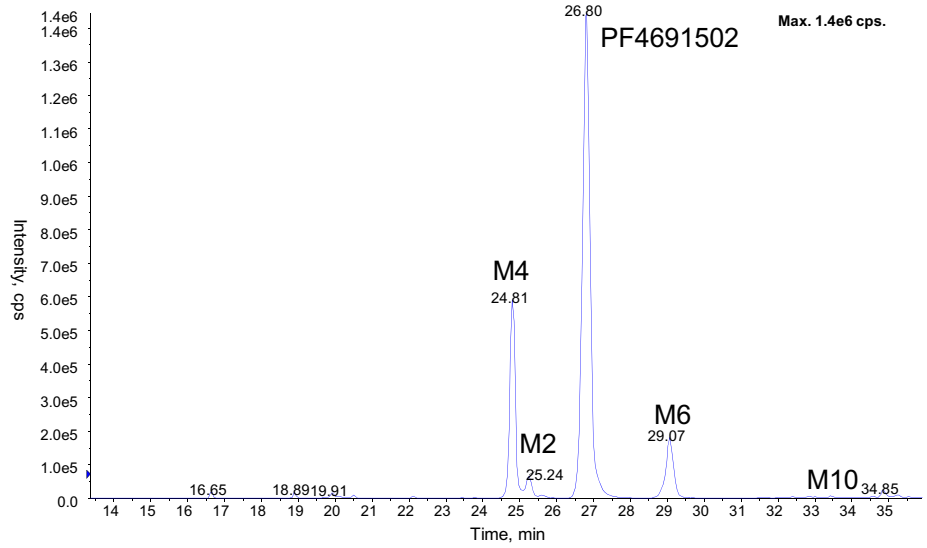

Figure 4. TIC of PF-04691502 and metabolites from FIP plasma sample.

4-MeO-5-F-3-pridine, hence increasing binding affinity. Indeed, **29** exhibits significant increase in mPI3Kα K_i over the corresponding des-F compound **28**. In an mTOR kinase assay, compounds with six-membered heterocycles such as **13** and **22** exhibit potent K_i. Interestingly, the most potent compound from the mTOR assay, **19**, has a pyrazole substituted at 6 position. When the pyrazole is methylated, the resultant compound **20** exhibits ninefold decrease in mTOR K_i, suggesting that the pyrazole N–H in **19** forms a H bond in the mTOR binding site. The lack of crystal structure of mTOR complex makes it difficult to explain the observed SAR at the molecular level. Figure 6 also shows there is no correlation between mPI3Kα K_i and mTOR K_i.

With regarding to physical properties, compounds discussed in the manuscript exhibit a wide range of calculated SFLogD (−0.35 to 2.65) and PSA (116–161). All the compounds, except the *cis*-cyclohexyl alcohols, are stable to in vitro oxidative clearance in HLM clearance studies, with Cl_{int} <8 μl/min/mg. When cell IC_{50} for both alcohol and amide derivatives is plotted against mPI3Kα K_i, mTOR K_i, PSA, RRCK, or calculated SFLogD, correlation is only seen between Cell IC_{50} and mPI3Kα K_i, as illustrated in Figure 7. Both *trans*-cyclohexyl alcohol **17** and *trans* cyclohexyl amide **29**, with 4-MeO-5-F-3-pyridine at 6 position, exhibit excellent cell potency, with IC_{50} of 5.24 and 5.82 nM, respectively. The metabolite **10** demonstrates potent K_i against mPI3Kα and mTOR, however, it

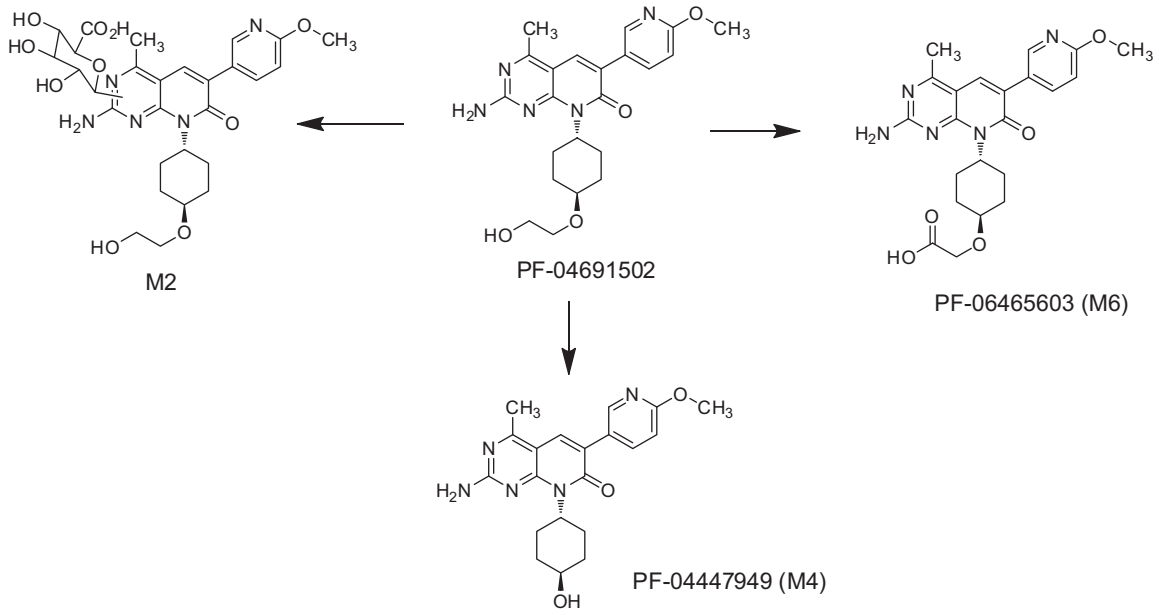

Figure 5. Metabolites identified from FIP day 21 plasma samples.

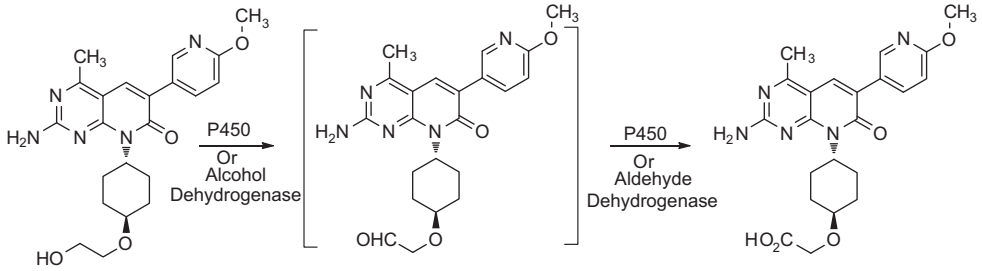

Scheme 2. Proposed pathway for the formation of the carboxylic acid metabolite (PF-06465603).

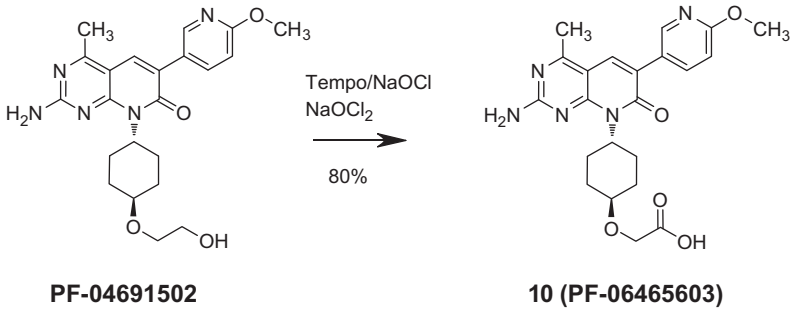

Scheme 3. Synthesis of **10** (PF-06465603).

exhibits weak cell potency with IC_{50} of 2.07 μM. At physiological pH, its terminal carboxylic acid is deprotonated, unable to form the corresponding intramolecular H bond that is present in the alcohol and the amide derivatives, therefore exhibiting poor permeability, with RRCK value of 0.295×10^{-6} cm/s, and weak cell potency.

Figure 7 illustrates that there is no correlation between cell IC_{50} and PSA for the compounds discussed in this paper; some compounds with high PSA exhibits excellent cellular activity. For example, PSA for **29** is 148 Å, and cell IC_{50} is 5.82 nM. This can be explained by the formation of the intramolecular H bond between the ether oxygen atom off the cyclohexyl and the N–H from the terminal amide. Farwell developed a method to measure the effective polar surface area (ePSA), which measures the exposed polarity of a molecule in a non-polar environment, and is reflective of both the intramolecular H bond and the size of molecules.[12] ePSA was determined for 13 compounds from Table 2, including both terminal alcohol and terminal amide derivatives. Even though there is no direct correlation between ePSA and PSA as illustrated in Figure 8, formation of intramolecular H bond can significantly reduce the effective polar surface area. Several compounds, with PSA greater than 135 Å, exhibits ePSA between 82 and 101 Å, which is a range capable of yielding excellent permeability and cellular potency. This suggests that, for designs with high PSA,

Table 1
SAR summary for MPP derivatives

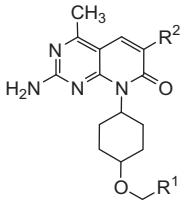

	cis/*trans*[a]	R^1	R^2	mPI3Ka K_i[b] (nM)	mTOR K_i[b] (nM)	Cell[b] IC_{50} (nM)	cSFLogD	HLM Cl_{int} (μl/min/mg)	RRCK (10^{-6} cm/s)	TPSA	ePSA[c]
10	*trans*	–COOH	4-MeO-3-pyridine	0.350	8.63	2070	−0.347	<8.00	0.295	142	99
11	*cis*	–OH	4-MeO-3-pyridine	4.51	12.8	21.6	2.3	55.7	19.3	125	77
12	*cis*	–OH	4-MeO-5-F-3-pyridine	1.18	ND	ND	2.44	142	17.9	125	76
13	*cis*	–OH	4-MeO-3-pyrimidine	2.41	4.46	29.4	1.47	18		138	82
14	*cis*	–OH	3-Pyrazole	13.5	7.50	11.2	1.42	23.4	12.6	132	95
15	*cis*	–OH	3-Me-3-pyrazole	26.4	45.9	310	1.43	13.3	23.3	121	78
16	*cis*	–OH	3-Quinoline	24.1	10.7	104	2.65	105	41.6	116	88
17	*trans*	–OH	4-MeO-5-F-3-pyridine	0.654	24.4	5.24	2.44	<8		125	
18	*trans*	–OH	4-MeO-3-pyrimidine	1.00	5.05	22.0	1.47	<8	21.3	138	87
19	*trans*	–OH	3-Pyrazole	3.44	2.15	25.9	1.42	<8		132	101
20	*trans*	–OH	3-Me-3-pyrazole	10.1	19.5	288	1.43	<8		121	
21	*trans*	–OH	3-Quinoline	8.01	7.82	23.8	2.65	<8	19.7	116	
22	*cis*	$–CONH_2$	4-MeO-3-pyridine	1.67	2.54	23.3	1.67	<8	30.3	148	85
23	*cis*	$–CONH_2$	4-MeO-5-F-3-pyridine	0.700	45.4	8.22	1.9	<8	26.2	148	85
24	*cis*	$–CONH_2$	4-MeO-3-pyrimidine	1.82	12.6	82.9	0.991	<8	30.1	161	
25	*cis*	$–CONH_2$	3-Pyrazole	6.89	4.52	148	1.33	<8	0.151	155	
26	*cis*	$–CONH_2$	3-Me-3-pyrazole	24.8	92.6	988	0.942	<8		144	
27	*cis*	$–CONH_2$	3-Quinoline	7.41	48.0	116	2.38	<8	4.57	139	97
28	*trans*	$–CONH_2$	4-MeO-3-pyridine	1.91	29.5	19.3	1.67	<8	4.58	148	
29	*trans*	$–CONH_2$	4-MeO-5-F-3-pyridine	0.312	11.1	5.82	1.9	<8	26.2	148	
30	*trans*	$–CONH_2$	4-MeO-3-pyrimidine	1.82	8.80	51.9	0.991	<8	29.8	161	
31	*trans*	$–CONH_2$	3-Pyrazole	6.16		256	1.3311			155	
32	*trans*	$–CONH_2$	3-Me-3-pyrazole	21.8		376	0.942			144	
33	*trans*	$–CONH_2$	3-Quinoline	5.74	9.10	56.8	2.28	<8	9.02	139	101

[a] Relative sterochemistry of the two substituents on cyclohexyl.
[b] Inhibition constants (K_i) and cell IC_{50} were determined as described in Refs. 5,6. The coefficients of variance were typically less than 20% ($n = 2$).
[c] Effective polar surface area.[12]

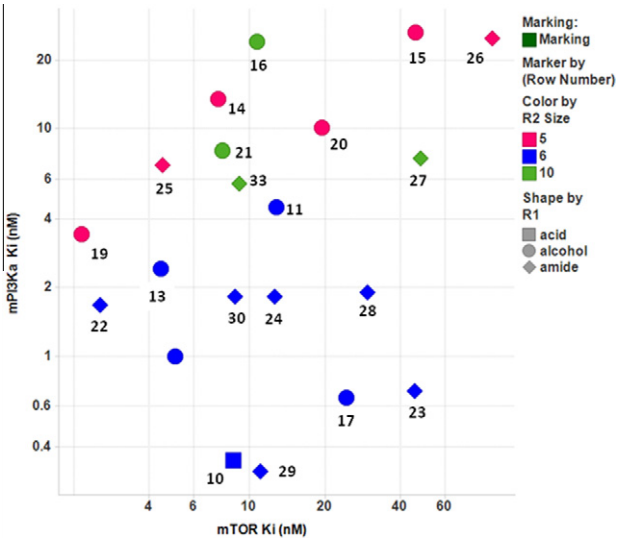

Figure 6. mPI3Kα K_i versus mTOR K_i plot.

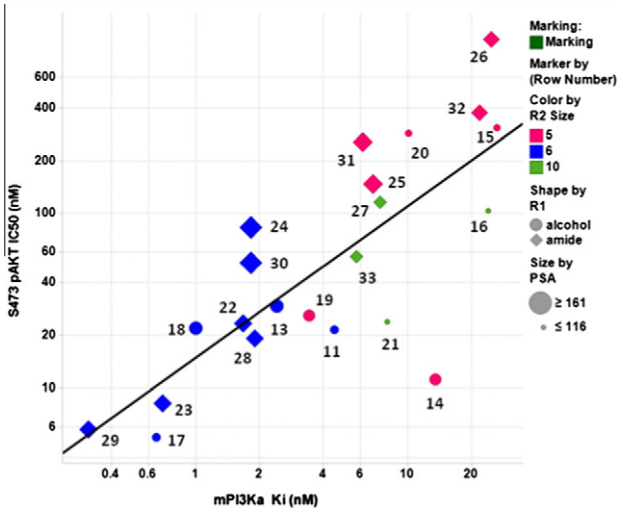

Figure 7. Correlation between S473 Cell IC_{50} versus mPI3Kα K_i.

introduction of an intramolecular H bond can help achieve good permeability and cellular potency by modulating ePSA to a desirable range.

Compound **17**, exhibiting excellent overall properties such as very good in vitro potency and low HLM clearance, was progressed to in vivo experiments including rat PK and mouse xenograft tumor growth inhibition efficacy studies. Compound **17** demonstrated excellent rat PK profile, with clearance of 17.0 ml/min/kg, V_{dss} of 4.08 L/kg, $T_{1/2}$ of 2.77 h, and 79% oral bioavailability. In TGI studies, **17** exhibited dose dependent efficacy in U87 xenograft model, demonstrating 89% TGI at the MTD of 10 mg/kg (Fig. 9).[6] Figure 10 shows that a robust in vivo PK/PD correlation for **17** was observed for samples from the high dose treatment group in the TGI studies. At 1 h time pint, high free drug concentration in plasma yielded

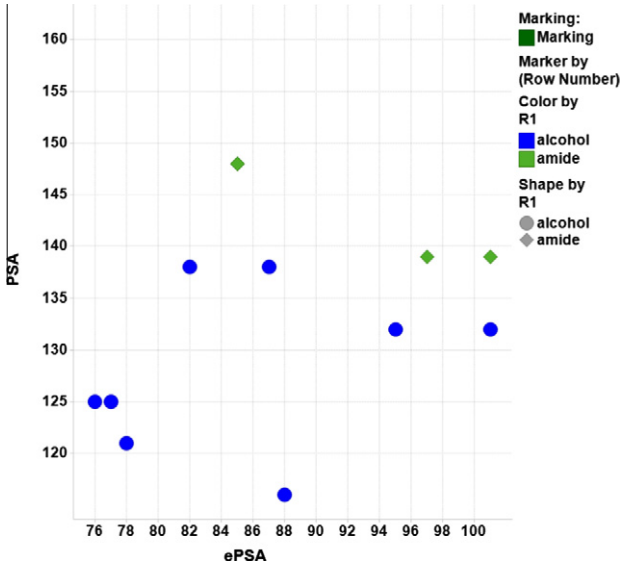

Figure 8. Correlation between PSA and ePSA.

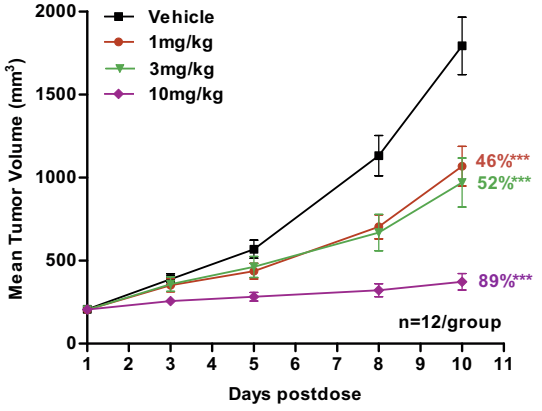

Figure 9. Tumor growth inhibition by 17 in U87MG mouse xenograft model (*** represents p <0.001).

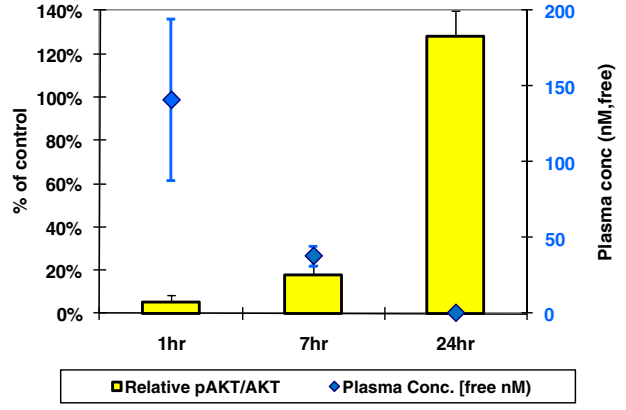

Figure 10. PK/PD correlation for 17 dosed at 10 mg/kg.

maximum inhibition of AKT phosphorylation. At 24 h time point, very low free drug concentration in plasma was correlated with minimum inhibition of AKT phosphorylation.

In summary, the MPP derivatives, including PF-06465603, a metabolite from human clinical trial of PF-04691502, demonstrated potent K_i in both mPI3Kα and mTOR in vitro assays. Even though calculated PSA was very high for the terminal alcohol and terminal amide MPP derivatives, the formation of the intramolecular H bond helped them to exhibit ePSA in a range to achieve good permeability and good cellular activity. Compound **17** (PF-04691503),[13] demonstrating excellent in vitro potency and robust ADMET properties, was progressed to in vivo antitumor efficacy model, and exhibited robust tumor growth inhibition.

Acknowledgments

John Almaden, Tom Carlson, Hieu Lam, Jeff Wang, Peter Wells, and Aihua Zou are acknowledged for biochemical screenings. Jeffrey Chen, Jon Engebretsen, and John Li are acknowledged for cellular screening. Jason Zbieg is acknowledged for synthesis assistance.

Supplementary data

Supplementary data associated with this article can be found, in the online version, at http://dx.doi.org/10.1016/j.bmcl.2013.02.020.

References and notes

1. Eagleman, J. A.; Luo, J.; Cantley, L. C. *Nat. Rev. Genet.* **2006**, *7*, 606.
2. Samuels, Y.; Wang, Z.; Bardelli, A.; Silliman, N.; Ptak, J.; Szabo, S.; Yan, H.; Gazdar, A.; Powell, S. M.; Riggins, G. J.; Willson, J. K. V.; Markowitz, S.; Kinzler, K. W.; Vogelstein, B.; Velculescu, V. E. *Science* **2004**, *304*, 554.
3. Shuttleworth, S. J.; Silva, F. A.; Cecil, A. R. L.; Tomassi, C. D.; Hill, T. J.; Raynaud, F. I.; Clarke, P. A.; Workman, P. *Curr. Med. Chem.* **2011**, *18*, 2686.
4. Courtney, K. D.; Corcoran, R. B.; Engelman, J. A. *J. Clin. Oncol.* **2008**, *28*, 1075.
5. Cheng, H.; Bagrodia, S.; Bailey, S.; Edwards, M.; Hoffman, J.; Hu, Q.; Kania, R.; Knighton, D. R.; Marx, M. A.; Ninkovic, S.; Sun, S.; Zhang, E. *MedChemCommun* **2010**, *1*, 139. Experimental procedures for in vitro biochemical assays and cellular assay were reported in this reference..
6. Yuan, J.; Mehta, P. P.; Yin, M.; Sun, S.; Zou, A.; Chen, J.; Rafidi, K.; Feng, Z.; Nickel, J.; Engebetsen, J.; Hallin, J.; Blasina, A.; Zheng, E.; Nguyen, L.; Sun, M.; Vogt, P. K.; McHarg, A.; Cheng, H.; Christensen, J. G.; Kan, J. L. C.; Bagrodia, S. *Mol. Cancer Ther.* **2011**, *10*, 2189. Experimental procedures for PK/PD and TGI studies were reported in this reference.
7. A crystal structure of a 4-MeO-5-F-3-pyridine MPP derivative with PI3Kγ was reported in the following reference. The movement of the Lys 833 side chain, and the H bonds between the Lys 833 terminal amino group and the MeO and F were present in the crystal structure Le, P. T.; Cheng, H.; Ninkovic, S.; Plewe, M.; Huang, X.; Wang, H.; Bagrodia, S.; Sun, S.; Knighton, D. R.; LaFleur, R.; Caroline, M. *Bioorg. Med. Chem. Lett.* **2012**, *22*, 5098.
8. Norman, M. H.; Andrews, K. L.; Bo, Y. Y.; Booker, S. K.; Caenepeel, S.; Cee, V. J.; D'Angelo, N. D.; Freeman, D. J.; Herberich, B. J.; Hong, F.; Jackson, C. L. M., et al *J. Med. Chem.* **2012**, *55*, 7796.
9. Cheng, H.; Bhumralkar, D.; Dress, K. R.; Hoffman, J. E.; Johnson, C. M.; Kania, R. S.; Le, P. T. Q.; Nambu, M. D.; Pairish, M. A.; Plewe, M. B.; Tran, K. T. Pyrido (2,3) pyrimidinone compounds and their use as PI3 inhibitors, WO 2008/032162.
10. Hamilton, R. A.; Garnett, W. R.; Kline, B. J. *Clin. Pharmacol. Ther.* **1981**, *29*, 408.
11. Biological activity for PF-04447949 was discussed in Ref. 5.
12. Farrell, W.; Masters-Moore, D.; Murphy, S.; Lafontaine, J. HPLC 2010 Symposium, Boston, MA, June 23, 2010, Oral Presentation. Manuscript describing the ePSA protocol is in preparation by Farrell.
13. Berlinski, P.; Kamerling, S.; Colhoun, H.; Forester, N.; Marotti, K.; Bagrodia, S.; Cheng, H.; Pascual, B.; Yuan, J.; Chen, J.; Engebretse, J.; Rafidi, K.; Zhang, E.; Wang, S.; Zou, A.; Carlson, T.; Almaden, C.; Barker, J.; Gehring, M.; Nguyen, L.; Shen, A.; Hemkens, M.; McHarg, A.; Sun, S.; Carley, W. 2010 AACR poster abstract # 5043, Washington DC, USA.